

The Journal of Physiology

A Nav1.7 channel mutation associated with hereditary erythromelalgia contributes to neuronal hyperexcitability and displays reduced lidocaine sensitivity

Patrick L. Sheets, James O. Jackson, II, Stephen G. Waxman, Sulayman D. Dib-Hajj
and Theodore R. Cummins

J. Physiol. 2007;581;1019-1031; originally published online Apr 12, 2007;

DOI: 10.1113/jphysiol.2006.127027

This information is current as of June 16, 2008

This is the final published version of this article; it is available at:

<http://jp.physoc.org/cgi/content/full/581/3/1019>

This version of the article may not be posted on a public website for 12 months after publication unless article is open access.

The Journal of Physiology Online is the official journal of The Physiological Society. It has been published continuously since 1878. To subscribe to *The Journal of Physiology Online* go to: <http://jp.physoc.org/subscriptions/>. *The Journal of Physiology Online* articles are free 12 months after publication. No part of this article may be reproduced without the permission of Blackwell Publishing: JournalsRights@oxon.blackwellpublishing.com

A Na_v1.7 channel mutation associated with hereditary erythromelalgia contributes to neuronal hyperexcitability and displays reduced lidocaine sensitivity

Patrick L. Sheets¹, James O. Jackson II¹, Stephen G. Waxman^{2,3,4}, Sulayman D. Dib-Hajj^{2,3,4} and Theodore R. Cummins¹

¹Department of Pharmacology and Toxicology, Stark Neurosciences Research Institute, Indiana University School of Medicine, Indianapolis, IN 46202, USA

²Department of Neurology and ³Center for Neuroscience and Regeneration Research, Yale University School of Medicine, New Haven, CT 06510, USA

⁴Rehabilitation Research Center, Veterans Administration Connecticut Healthcare System, West Haven, CT 06516, USA

Mutations in the TTX-sensitive voltage-gated sodium channel subtype Na_v1.7 have been implicated in the painful inherited neuropathy, hereditary erythromelalgia. Hereditary erythromelalgia can be difficult to treat and, although sodium channels are targeted by local anaesthetics such as lidocaine (lignocaine), some patients do not respond to treatment with local anaesthetics. This study examined electrophysiological differences in Na_v1.7 caused by a hereditary erythromelalgia mutation (N395K) that lies within the local anaesthetic binding site of the channel. The N395K mutation produced a hyperpolarized voltage dependence of activation, slower kinetics of deactivation, and impaired steady-state slow inactivation. Computer simulations indicate that the shift in activation is the major determinant of the hyperexcitability induced by erythromelalgia mutations in sensory neurons, but that changes in slow inactivation can modulate the overall impact on excitability. This study also investigated lidocaine inhibition of the Na_v1.7-N395K channel. We show that the N395K mutation attenuates the inhibitory effects of lidocaine on both resting and inactivated Na_v1.7. The IC₅₀ for lidocaine was estimated at 500 μM for inactivated wild-type Na_v1.7 and 2.8 mM for inactivated Na_v1.7-N395K. The N395K mutation also significantly reduced use-dependent inhibition of lidocaine on Na_v1.7 current. In contrast, a different hereditary erythromelalgia mutation (F216S), not located in the local anaesthetic binding site, had no effect on lidocaine inhibition of Na_v1.7 current. Our observation of reduced lidocaine inhibition on Na_v1.7-N395K shows that the residue N395 is critical for lidocaine binding to Na_v1.7 and suggests that the response of individuals with hereditary erythromelalgia to lidocaine treatment may be determined, at least in part, by their specific genotype.

(Resubmitted 21 December 2006; accepted after revision 2 April 2007; first published online 12 April 2007)

Corresponding author T. R. Cummins: Department of Pharmacology and Toxicology, Stark Neurosciences Research Institute, Indiana University School of Medicine, 950 West Walnut St, R2 468, Indianapolis, IN 46202, USA.

Email: trcummin@iupui.edu.

Primary hereditary erythromelalgia is an inherited autosomal dominant painful neuropathy that is marked by intense burning pain and redness of the extremities (van Genderen *et al.* 1993). Mutations in the *SCN9A* gene (chromosome 2) encoding for TTX-sensitive voltage-gated sodium channel subtype Na_v1.7 have been implicated in primary hereditary erythromelalgia (Yang *et al.* 2004; Drenth *et al.* 2005). Na_v1.7 is expressed at high levels in rat and human dorsal root ganglia (DRG) and

sympathetic ganglia (Black *et al.* 1996; Toledo-Aral *et al.* 1997; Sangameswaran *et al.* 1997) and is a transmembrane protein that responds to small, slow depolarizations and contributes to action potential generation. Na_v1.7 is known to be expressed abundantly in nociceptive neurons (Djoughri *et al.* 2003). Electrophysiological studies have shown hyperpolarized voltage dependence of activation, slower deactivation kinetics, and larger ramp currents in Na_v1.7 with the I848T, L858H, L858F mutations implicated in hereditary erythromelalgia (Cummins *et al.* 2004; Han *et al.* 2006). The L858H mutation is known to make DRG neurons hyperexcitable, while making

This paper has online supplemental material.

sympathetic ganglion neurons hypoexcitable (Rush *et al.* 2006). DRG neurons transfected with several other $\text{Na}_v1.7$ mutations implicated in hereditary erythromelgia (F1449V, A863P) have a lower threshold for firing action potentials and fire at higher-than-normal frequencies in response to suprathreshold stimulation (Dib-Hajj *et al.* 2005; Harty *et al.* 2006). A recent study has shown that a family affected by paroxysmal extreme pain disorder (PEPD), characterized by rectal, ocular and submandibular pain, have missense mutations in the SCN9A gene encoding for $\text{Na}_v1.7$ (Fertleman *et al.* 2006). Furthermore, there is new evidence showing that $\text{Na}_v1.7$ mutations that cause loss of function underlies a congenital disorder where the ability to experience pain is absent (Cox *et al.* 2006). Taken together, these studies indicate that changes in $\text{Na}_v1.7$ properties play a crucial role in the production of pain and suggest that hereditary erythromelgia mutations could serve as a model for examining changes in voltage-gated sodium channels that may contribute to pain in humans.

One hereditary erythromelgia mutation that has been associated with a very severe phenotype is the N395K $\text{Na}_v1.7$ mutation (Drenth *et al.* 2005), located in the S6 segment of domain I. The residue corresponding to N395 in other voltage-gated sodium channels is involved in the interaction with local anaesthetics. Lysine substitution at the corresponding residue (N434K) in the rat $\text{Na}_v1.4$ sodium channel reduces local anaesthetic block of $\text{Na}_v1.4$ (Nau *et al.* 1999). Therefore, we predicted that the N395K mutation in $\text{Na}_v1.7$ alters interaction of local anaesthetics with the channel. Unfortunately both of the affected individuals in the original family with the N395K mutation (Drenth *et al.* 2005) are now deceased and data on sensitivity of these patients to local anaesthetics is not available. Interestingly, one study has shown that treatment of erythromelgia with lidocaine relieves pain in only 55% of afflicted patients (Davis & Sandroni, 2005). Due to the multiple mutations involved in hereditary erythromelgia, it is possible that some but not all of these mutations alter local anaesthetic binding to $\text{Na}_v1.7$, and this may contribute to the variability in patients responding to lidocaine. Therefore, the goals of this study were to (1) examine electrophysiological changes in $\text{Na}_v1.7$ produced by the N395K mutation and how they affect the excitability of a model sensory neuron and (2) determine if the N395K mutation in $\text{Na}_v1.7$ changes the effects of lidocaine on sodium channel current.

Methods

Transfections

The human $\text{Na}_v1.7$ (wild-type, N395K, or F216S) channels were cotransfected with the human $\beta 1$ and $\beta 2$ subunits into human embryonic kidney (HEK293) cells using

the calcium phosphate precipitation technique. The N395K and F216S mutations were produced using the QuickChange XL Site-Directed Mutagenesis Kit (Stratagene; La Jolla, CA, USA). HEK293 cells were grown under standard tissue culture conditions (5% CO_2 ; 37°C) in Dulbecco's modified Eagle's medium (DMEM) supplemented with 10% fetal bovine serum. The calcium phosphate–DNA mixture was added to the cell culture medium and left for 3 h, after which the cells were washed with fresh medium. Sodium currents were recorded 40–72 h after transfection.

Chemicals and solutions

Lidocaine hydrochloride (Sigma Aldrich, St Louis, MO, USA) was dissolved in standard bathing solution to give a stock solution of 100 mM. Subsequent dilutions were performed in standard bathing solution to give concentrations of (mM): 0.1, 0.3, 1, 3, 10 and 30. Lidocaine solutions were made fresh before patch-clamp recordings.

Whole-cell patch-clamp recordings

Whole-cell patch-clamp recordings were conducted at room temperature ($\sim 21^\circ\text{C}$) using a HEKA EPC-10 amplifier. Data were acquired on a Windows-based Pentium IV computer using the Pulse program (v 8.65, HEKA Electronic, Germany). Fire-polished electrodes (0.9–1.3 M Ω) were fabricated from 1.7 mm capillary glass using a Sutter P-97 puller (Novato, CA, USA). The standard pipette solution contained (mM): 140 CsF, 10 NaCl, 1.1 EGTA and 10 Hepes, pH 7.3. The standard bathing solution contained (mM): 140 NaCl, 1 MgCl₂, 3 KCl, 1 CaCl₂ and 10 Hepes, pH 7.3 (adjusted with NaOH). Cells on glass coverslips were transferred to a recording chamber containing 250 μl of standard bathing solution. Protocols were performed 4 min after whole-cell configuration had been established to allow for adequate equilibration of the intracellular solution. Lidocaine solutions were added to the bath compartment by first withdrawing 25 μl of bathing solution, then adding 25 μl of 10-fold concentrated lidocaine and mixing 10–15 times with a 100 μl pipettor. Final concentrations of lidocaine in the bath compartment were in the range of 10 μM to 10 mM. Series resistance errors were compensated to be less than 3 mV during voltage-clamp recordings.

Data analysis

Voltage clamp experimental data were analysed using the Pulsefit (v 8.65, HEKA Electronic), Origin (OriginLab Corp., Northampton, MA, USA), and Microsoft Excel software programs. Slope factors of conductance–voltage and steady-state inactivation curves were calculated using

the general Boltzmann function:

$$I(V) = \text{Offset} + \left[\frac{\text{Amplitude}}{1 + \exp(-(V - V_{\text{half}})/\text{Slope})} \right]$$

The equations used for the one-site binding curve and two-site binding curves for the dose–inhibition relationship for lidocaine and the Na_v channels were as follows:

One-site binding curve:

$$v = \frac{[\text{Lidocaine}]_{\text{free}}}{[\text{Lidocaine}]_{\text{free}} + K_d}$$

Two-site binding curve:

$$v = \frac{[\text{Lidocaine}]_{\text{free}}}{[\text{Lidocaine}]_{\text{free}} + K_{d1}} + \frac{[\text{Lidocaine}]_{\text{free}}}{[\text{Lidocaine}]_{\text{free}} + K_{d2}}$$

Computer simulations

The electrical properties of small sensory neurons were simulated using the NEURON program (version 5.9) (Hines & Carnevale, 1997). Sodium and potassium conductances were modelled as described below using Hodgkin & Huxley-type (HH) descriptions (Hodgkin & Huxley, 1952) of the various voltage-dependent currents. Action potential firing was simulated using a single compartment cylindrical model of length 37.75 μm and radius 20 μm, simulating a small sensory neuron with a 3000 μm² surface area and 24.3 pF capacitance. The integration method was Backward Euler at an integration time step *dt* of 0.025 ms.

Simulations were performed assuming free ionic concentrations of sodium ([Na⁺]_o = 145 mM; [Na⁺]_i = 12 mM) and potassium ([K⁺]_o = 8 mM; [K⁺]_i = 118 mM) which were used to calculate their Nernst reversal potential of +63.4 mV (*E*_{Na}) and –68.5 mV (*E*_K), respectively. By analogy to the HH model of action potential electrogenesis, the linear leakage current was defined as *I*_{Leak} = *g*_{Leak}(*V* – *E*_{Leak}), where *g*_{Leak} is the leak conductance, *V* is the membrane potential, and *E*_{Leak} is the reversal potential for the leak current. *E*_{Leak} was set at –55 mV. The size of the current was adjusted so that its amplitude corresponded to an input resistance of 706 MΩ: *g*_{Leak} = 0.000425 S cm^{–2}, similar to that reported for small sensory neurons (Wang *et al.* 2005).

The DRG neuron model included a leak conductance, two potassium conductances, Na_v1.7 conductance(s) (wild-type and mutant) and Na_v1.8, slowly inactivating TTX-R conductance. The predominant potassium conductances in small DRG neurons are a sustained (delayed rectifier type) conductance and a transient (A-type) conductance (Gold *et al.* 1996). Therefore we introduced into the model a delayed rectifier potassium

current (*I*_{KDR}) and an A-type potassium current (*I*_{KA}). The majority of small (< 25 μm diameter) DRG neurons exhibit both TTX-S and -R currents (Cummins & Waxman, 1997). Although many small DRG neurons express the mRNA for more than one TTX-S sodium channel isoform (Black *et al.* 1996), the major TTX-S current in the majority of small DRG neurons closely resembles the current produced by Na_v1.7 channels (Cummins *et al.* 1998). Therefore the only TTX-S conductances included in our model simulate Na_v1.7 currents. Both slowly inactivating (Na_v1.8-like) and persistent (Na_v1.9-like) TTX-R currents can be recorded from many small DRG neurons (Cummins *et al.* 1999). The persistent TTX-R current is subject to significant modulation and tends to be negligible when the cells are held at ~ –60 mV (Cummins *et al.* 1999) and therefore we only included the Na_v1.8-like TTX-R current in our model neuron. For specific details of the current models see online Supplemental material.

Results

The N395K mutation alters electrophysiological properties of Na_v1.7

Wild-type (WT) hNa_v1.7 or the mutant derivative channel N395K were transiently expressed with hβ-1 and hβ-2 subunits in HEK293 cells. An initial comparison of current traces from both channels did not suggest any major differences in channel kinetics (Fig. 1A and B). The voltage dependence of activation was measured for each channel using a series of depolarizing test pulses from –100 to +70 mV. N395K channels exhibited a hyperpolarized current–voltage (*I*–*V*) and conductance–voltage (*G*–*V*) curve compared to wild-type channels (Fig. 1C and D). The midpoint of activation (estimated using a Boltzmann function) was significantly (*P* < 0.001) more negative (–28.0 ± 1.1 mV; slope: 6.7 ± 0.1; *n* = 18) for N395K channels than for WT channels (–20.3 ± 0.8 mV; slope: 7.27 ± 0.1; *n* = 19; Student's unpaired *t* test). The voltage dependence of steady-state fast inactivation was also evaluated for each channel and, in contrast to activation, did not differ between the WT and mutant channels (Fig. 2A). The midpoint of steady-state fast inactivation for the WT channels (–71.3 ± 0.8 mV; slope: 6.79 ± 0.2; *n* = 19) was not significantly different (*P* = 0.76) from that of the N395K channels (–70.9 ± 1.1 mV; slope: 6.14 ± 0.1; *n* = 18; Student's unpaired *t* test).

Next, we examined whether the N395K mutation in Na_v1.7 had any effect on steady-state slow inactivation. Mutations impairing steady-state slow inactivation in voltage-gated sodium channels have been implicated in hyperkalaemic periodic paralysis, hereditary erythromelalgia, and epilepsy (Cummins &

Sigworth, 1996; Bendahhou *et al.* 1999, 2002; Cummins *et al.* 2004; Rhodes *et al.* 2005). It has further been shown that mutations in residues corresponding to N395 in the skeletal muscle $\text{Na}_v1.4$ channel (N434) and the brain $\text{Na}_v1.2$ channel (N418) alter slow inactivation (Wang & Wang, 1997; Nau *et al.* 1999; Chen *et al.* 2006). Steady-state slow inactivation was tested by holding the cells at -120 mV and stepping to an inactivating pre-pulse (ranging from -130 to 10 mV) for 30 s. This was followed by a 100 ms pulse to -120 mV to allow recovery from fast inactivation and a test pulse to -10 mV for 25 ms to assess the fraction of current remaining available for activation. The change in channel availability measured with this protocol reflects the fraction of channels that undergo slow inactivation. N395K channels showed an impaired steady-state slow inactivation compared to WT channels (Fig. 2B). The midpoint of steady-state slow inactivation for N395K channels (-33.6 ± 2.6 mV; slope: 11.8 ± 0.2 ; $n = 6$) was significantly ($P < 0.01$) depolarized compared to WT channels (-46.7 ± 1.7 mV; slope: 16.1 ± 1.0 ; $n = 6$; Student's unpaired t test).

The kinetics of deactivation for WT and N395K channels was also examined by eliciting tail currents at

a range of potentials after brief activation of the channels (-20 mV for 0.5 ms). Deactivation reflects the transition of the channel from the open to the closed state, and defects in skeletal muscle sodium channel deactivation have been implicated in paramyotonia congenita (Featherstone *et al.* 1998). The time constant of deactivation (measured with single exponential fits) was slower for the N395K channel than that of the WT channel at potentials ranging from -100 mV to -40 mV (Fig. 2C). The change in the kinetics of deactivation is consistent with the shift in the voltage dependence of activation.

A computer model of a sensory neuron expressing the electrophysiological properties of the N395K channel displays increased excitability

Our data show that the N395K mutation has two predominant effects on channel gating: it shifts the voltage dependence of activation in the negative direction and impairs slow inactivation of $\text{Na}_v1.7$ channels. To investigate how these alterations in sodium channel gating influence action potential firing, we simulated sensory neuron membrane conductances and firing

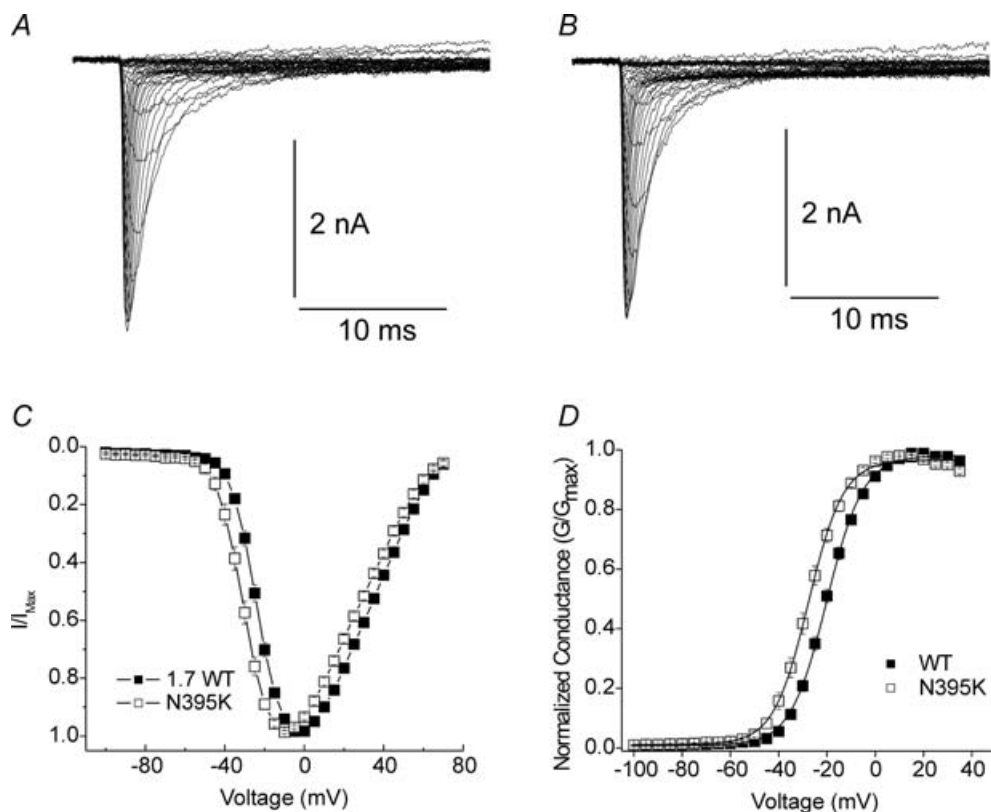


Figure 1. Comparison of electrophysiological properties between WT and N395K $\text{Na}_v1.7$ channels
A and B, current–voltage (I – V) traces for HEK293 cells transfected with WT (A) and N395K (B) channels. Both channels were coexpressed with the human β_1 and β_2 subunits. C and D, the I – V relationship (C) and steady-state activation curve (D) for N395K was hyperpolarized compared to WT.

properties in the single compartment model using the NEURON modelling program (Hines & Carnevale, 1997). Hodgkin–Huxley-type simulations of Na_v1.7, Na_v1.8, a delayed rectifier potassium current and an A-type potassium current were developed based on our sodium current recordings and descriptions in the literature (Gold *et al.* 1996) to approximate voltage-gated channel behaviour (Fig. 3A–D). The effects of several different mutant conductances were simulated. An activation mutant had its voltage dependence of activation shifted in the negative direction by 10 mV. A negative shift in activation should theoretically increase window current amplitudes. In the model the –10 mV shift increased window currents from 0.05% to 0.2% of the peak current amplitude. A 0.2% window current has an amplitude of 5 pA for a peak current of 2.5 nA. Therefore, while the model does predict that the mutation induces an increase in window currents, a current this size would be difficult to measure experimentally in HEK293 cells. In the model we also simulated a slow-inactivation mutant that had its steady-state slow inactivation altered to mimic the effect of the N395K mutation on this parameter. The simulated N395K mutant conductance combined these two alterations (Fig. 3E). Finally, because some erythromelalgia mutants shift activation in the negative direction but enhance steady-state slow inactivation (Cummins *et al.* 2004; Choi *et al.* 2006) we also included a simulated conductance where activation was shifted in the negative direction by 10 mV and slow inactivation was enhanced by increasing the transition rates 2-fold and shifting the midpoint of steady-state slow inactivation by 16 mV in the negative direction. This combination approximates that observed with the F216S erythromelalgia mutation (Choi *et al.* 2006).

In the first series of simulations we examined the effects of substituting 50% of the wild-type Na_v1.7 current in the computer model with one of the mutant conductances on action potential firing in response to 1 s injections of current. With the pure wild-type Na_v1.7 conductance, the threshold for generation of single action potentials (tested at 5 pA increments) was elicited with a 100 pA current injection (Fig. 3F) and a train of action potentials could be elicited when current injections were greater than 350 pA (Fig. 4A). This behaviour was not altered by insertion of the mutant conductance with impaired slow inactivation (Fig. 4A). However, the mutant conductance in combination with the shifted activation decreased the threshold for action potential generation in the model cell to 60 pA and had profound effects on repetitive firing in the model neuron (Fig. 4A). Although altering slow inactivation of the Na_v1.7 conductance with wild-type activation did not seem to change firing properties in our model neuron, altering slow inactivation in combination with altering the voltage dependence of activation did dramatically modify action potential firing.

The F216S-like current, with hyperpolarized activation and enhanced slow inactivation, had a decreased impact on repetitive firing compared to the activation mutant with normal slow inactivation. In contrast, the N395K-like current, with hyperpolarized activation and impaired slow inactivation, fired dramatically increased numbers of

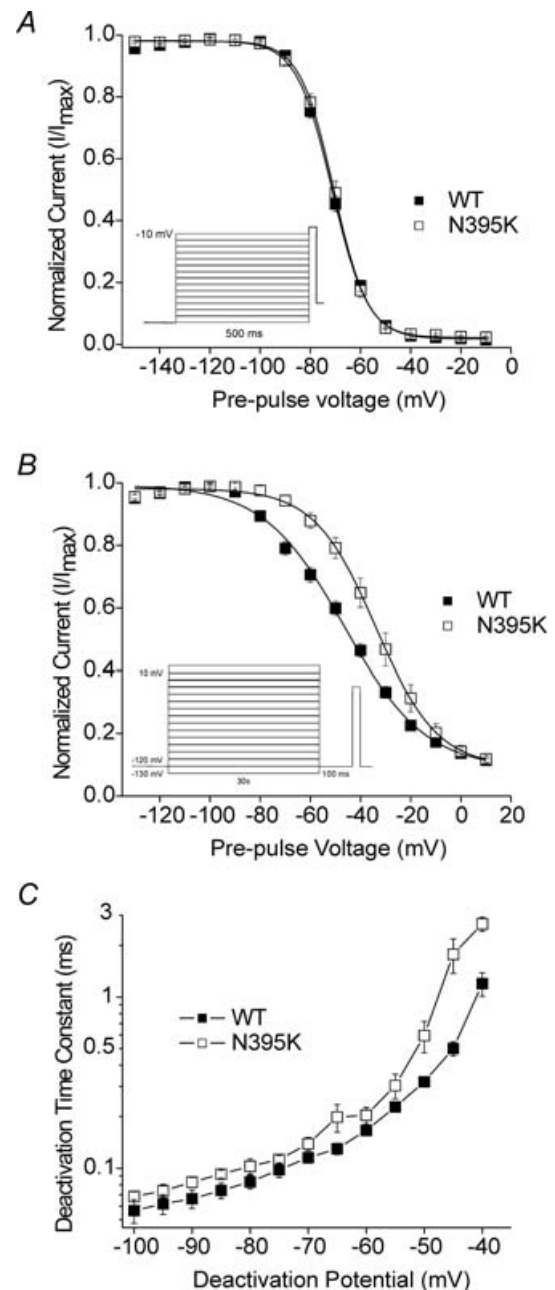


Figure 2. Comparison of inactivation and deactivation properties between WT and N395K channels

A, the steady-state fast inactivation curves for WT and N395K channels were not significantly different. B, the N395K channel showed an impaired steady-state slow inactivation curve compared to WT. C, N395K channels displayed a slightly slower onset of deactivation than that of WT.

action potentials with current injections ranging from 150 to 350 pA (Fig. 4A). The threshold for generation of single action potentials was also changed, with 65 pA required in the simulation with the F216S-like current and 55 pA required in the simulation with the N395K-like current.

In the second series of simulations we examined the ability of the model neuron to sustain action potential firing. With a 350 pA current injection lasting 10 s, only one action potential is observed in the simulation with 100% wild-type $\text{Na}_v1.7$ current (Fig. 4B). However, with 50% of the $\text{Na}_v1.7$ current having a hyperpolarized voltage dependence of activation, action potentials are generated throughout the 10 s (Fig. 4C). In the simulation with 50% of the $\text{Na}_v1.7$ current having only impaired slow inactivation, only a single action potential was again observed (Fig. 4D). The N395K-like current was able to induce firing throughout the 10 s simulation at approximately twice the frequency observed with the activation mutant with normal slow inactivation (Fig. 4E). This difference in firing frequency was sustained even with simulations where current injection lasted 180 s. In the simulation with the F216S-like conductance, firing was observed only during the first 2 s of the stimulation (Fig. 4F). Sustained repetitive firing could be observed with all of the different mutant $\text{Na}_v1.7$ channels at

higher levels of current injection (simulations not shown); however, the firing frequency was always higher with the N395K-like current than with the F216S-like current. This basic result was relatively insensitive to changes in current densities and was observed with several different formulations of the potassium conductances, suggesting that it is likely to reflect the relative impact of changes in activation and slow inactivation on sensory neuronal excitability. In the absence of $\text{Na}_v1.8$ current the model neuron did not fire repetitively, but the mutant channels did decrease the threshold for firing single action potentials. While these simulations are relatively simple, they indicate that the hyperpolarizing shift in voltage dependence of activation is a major determinant of hyperexcitability associated with the erythromelalgia mutations and suggest that the alterations in slow inactivation may play an important role in modulating the overall impact of the shift in activation on excitability.

The N395K mutation decreases $\text{Na}_v1.7$ sensitivity to lidocaine

Lysine substitution at the residue corresponding to N395 in rat skeletal muscle $\text{Na}_v1.4$ channel (N434) has been

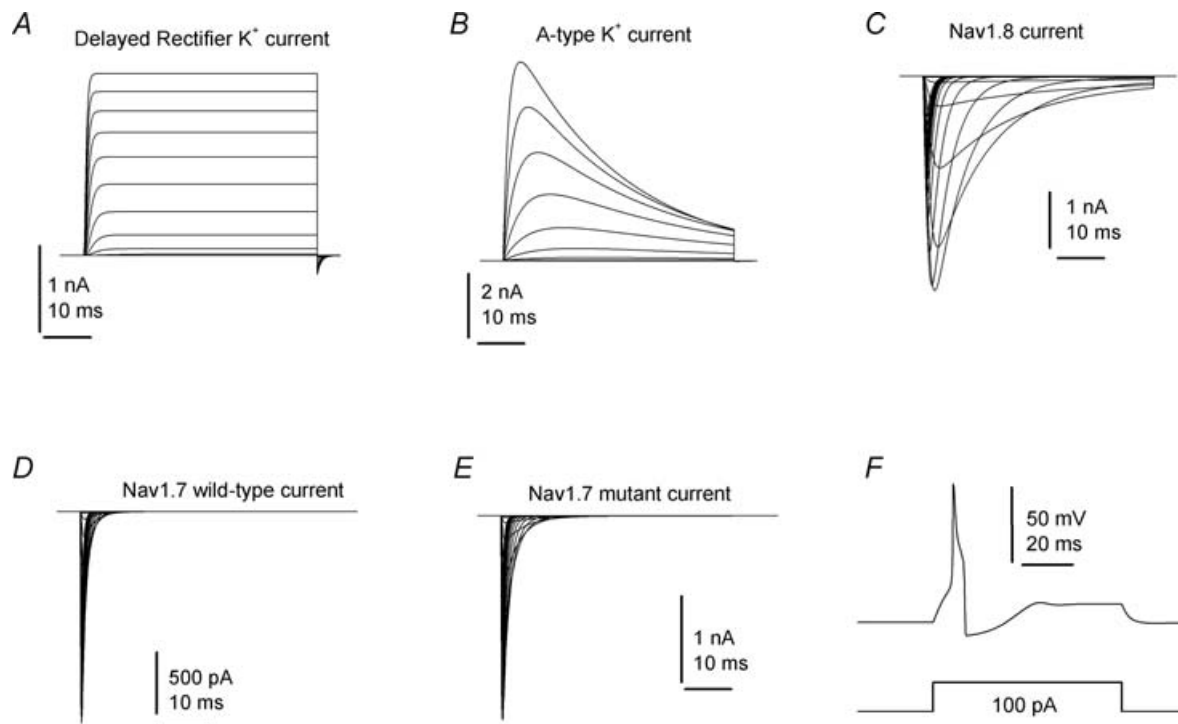


Figure 3. Simulated recordings from a model dorsal root ganglion (DRG) neuron

Voltage-clamp traces show the simulated delayed rectifier potassium current (A), A-type potassium current (B), $\text{Na}_v1.8$ current (C), wild-type $\text{Na}_v1.7$ current (D) and mutant $\text{Na}_v1.7$ current with hyperpolarized activation (E). The model cell was held at -80 mV and stepped to voltages between -80 and 50 mV. F, current-clamp simulation of the model cell containing leak current, delayed rectifier potassium current, A-type potassium current, $\text{Na}_v1.8$ current and wild-type $\text{Na}_v1.7$ current.

shown to reduce the affinity for both amitriptyline and local anaesthetics for inactivated channels (Nau *et al.* 1999; Wang *et al.* 2004; Nau & Wang, 2004). Therefore we tested the impact of the N395K mutation on local anaesthetic binding to Na_v1.7. Inhibition of channel current by a range of lidocaine concentrations (10 μ M to 10 mM) was examined for WT and N395K channels in the inactivated and resting state. Lidocaine binding to the inactivated state of the channels was tested by holding the cells at -120 mV and stepping to an inactivating pre-pulse (-50 mV) for 10 s, which is sufficient to inactivate all of the channels. This was followed by 100 ms pulses to -120 mV to allow recovery from fast inactivation, and the fraction of current remaining was measured in the absence and presence of lidocaine with a 20 ms test pulse to -10 mV.

Inhibition of channel current by lidocaine was attenuated for inactivated N395K channels compared to WT (Fig. 5A). Using a one-site binding fit, the IC₅₀ of lidocaine for inactivated WT channels was estimated at 500 μ M while the IC₅₀ for inactivated N395K channels was estimated at 2.8 mM. However, the one-site binding model did not produce a good fit for the dose–inhibition relationship of lidocaine and inactivated WT channels.

The data show that between 100 and 300 μ M, lidocaine inhibition of WT inactivated channels reaches a plateau before increasing at doses of 1 mM and higher (Fig. 5A). We hypothesized that this plateau in the relationship was due to more than one site being available for lidocaine binding. A two-site binding model gave a much better fit to the WT data. This fit indicated that there are possibly two populations of WT sodium channels at -50 mV, one that exhibits high affinity lidocaine binding while the other exhibits low affinity binding. Based on the two-site fit, the IC₅₀ of lidocaine for the high affinity and low affinity binding to WT channels was 210 μ M and 4.3 mM, respectively. The high affinity and low affinity populations may represent channels in different inactivated conformations (see Discussion). These data show that the N395K mutation significantly reduces lidocaine inhibition of Na_v1.7 channels at -50 mV, especially the high affinity binding.

Lidocaine binding to the resting state of the channels was tested by holding the cells at -120 mV and stepping to a pre-pulse of -140 mV for 10 s. The fraction of current remaining was assessed by a test pulse to -10 mV for 25 ms. Lidocaine had little or no effect on resting WT and N395K

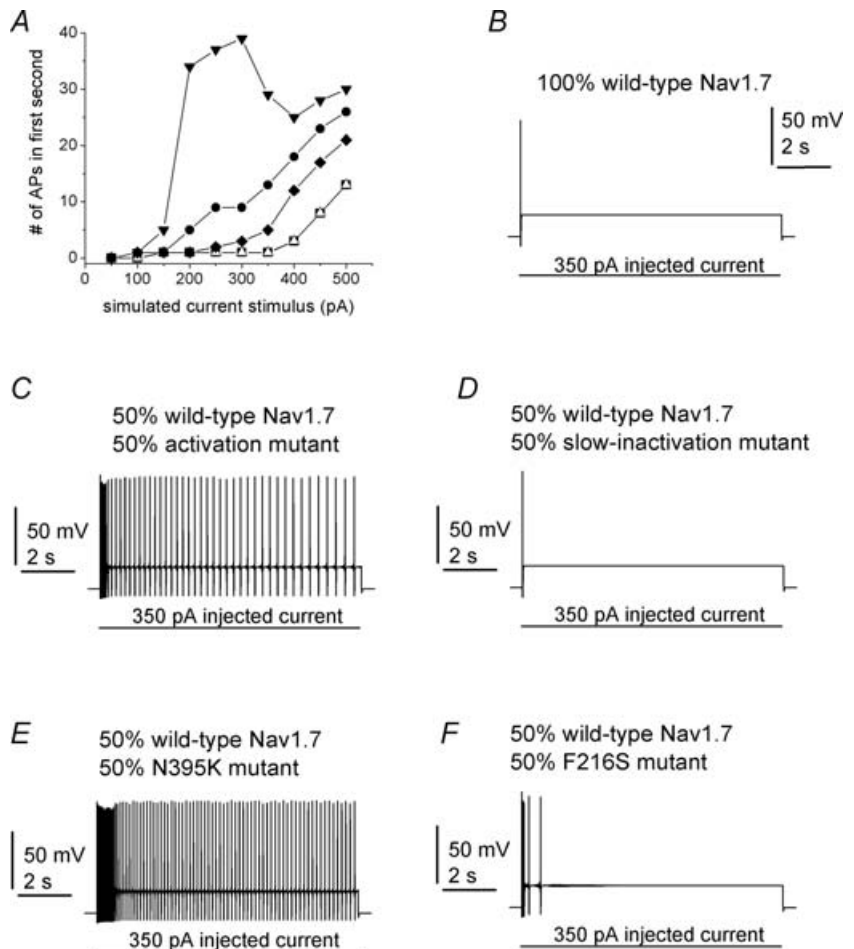


Figure 4. The effect of altering Na_v1.7 properties on repetitive action potential firing was simulated in a computer model of a DRG neuron

A, the number of action potentials generated in the model neuron in response to a 1 s current injection was measured. Current injections ranged from 50 to 500 pA. When the simulated neuron contained 100% wild-type Na_v1.7 (■) current only one action potential was generated for current injections of 100–350 pA. The response was virtually identical when 50% of the Na_v1.7 current had impaired slow inactivation (Δ). Repetitive firing was increased to different extents when 50% of the Na_v1.7 current had hyperpolarized activation (●), hyperpolarized activation combined with impaired slow inactivation (N395K mutant; ▼) or hyperpolarized activation combined with enhanced slow inactivation (F216S mutant; ◆). B–F, action potentials simulated in response to a 10 s injection of 350 pA are shown for the different combinations of Na_v1.7 wild-type and mutant currents.

channels at low concentrations (10 μM to 1 mM) while showing more inhibition at higher concentrations (3 mM, 10 mM) (Fig. 5B). Using a one-site binding fit, the IC_{50} of lidocaine for resting WT channels was estimated at 4.3 mM while the IC_{50} for resting N395K channels was estimated at 7.9 mM. In contrast to the inactivated channel data, a two-site binding model did not give a better fit to the WT resting channel data. These data indicate that the N395K mutation also reduces the inhibition of resting channels by lidocaine, although to a lesser extent than that shown at -50 mV.

As local anaesthetics are known to exhibit use-dependent inhibition of sodium currents, use-dependent effects of lidocaine on the WT and N395K channels were also studied. We investigated this by pulsing the transfected cells to -10 mV at a frequency of 5 Hz in the absence and presence of drug. Figure 6A and B displays examples of results under control conditions (left) and in

the presence of 300 μM lidocaine (right) for both the WT and N395K channels. WT current amplitude decreased $10.4 \pm 3.3\%$ ($n = 6$), $18.1 \pm 3.2\%$ ($n = 6$), $27.8 \pm 3.3\%$ ($n = 11$) and $42.7 \pm 2.0\%$ ($n = 7$) from the first pulse to the last pulse of the protocol in the presence of 10, 30, 100 and 300 μM lidocaine, respectively (Fig. 6C). Decreases in N395K current amplitude were significantly ($P < 0.01$) smaller (one-way ANOVA followed by Tukey's comparison test) at 30, 100 and 300 μM lidocaine (Fig. 6C). Decreases observed for the N395K channel were $2.4 \pm 0.6\%$ ($n = 6$), $1.7 \pm 0.6\%$ ($n = 5$), $4.3 \pm 0.6\%$ ($n = 6$) and $11.0 \pm 2.6\%$ ($n = 5$) for 10, 30, 100 and 300 μM lidocaine, respectively.

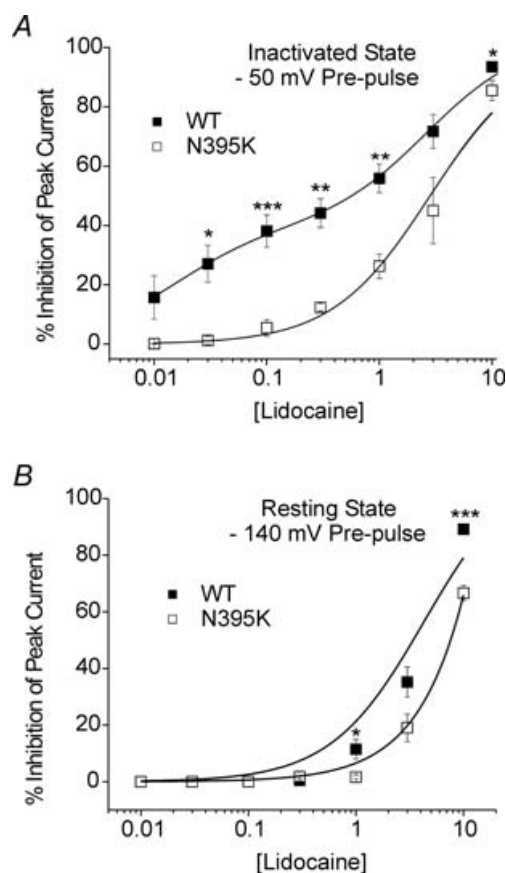


Figure 5. Effects of lidocaine on inactivated and resting WT and N395K channels

A, dose-response of lidocaine inhibition was attenuated on inactivated N395K channels at all concentrations of lidocaine tested compared to inactivated WT. **B**, dose-response of lidocaine inhibition was attenuated on resting N395K channels for 3 and 10 mM lidocaine compared to resting WT. Data are presented as mean percentage inhibition of peak current \pm s.e.m. (* $P < 0.05$, ** $P < 0.01$, *** $P < 0.001$.)

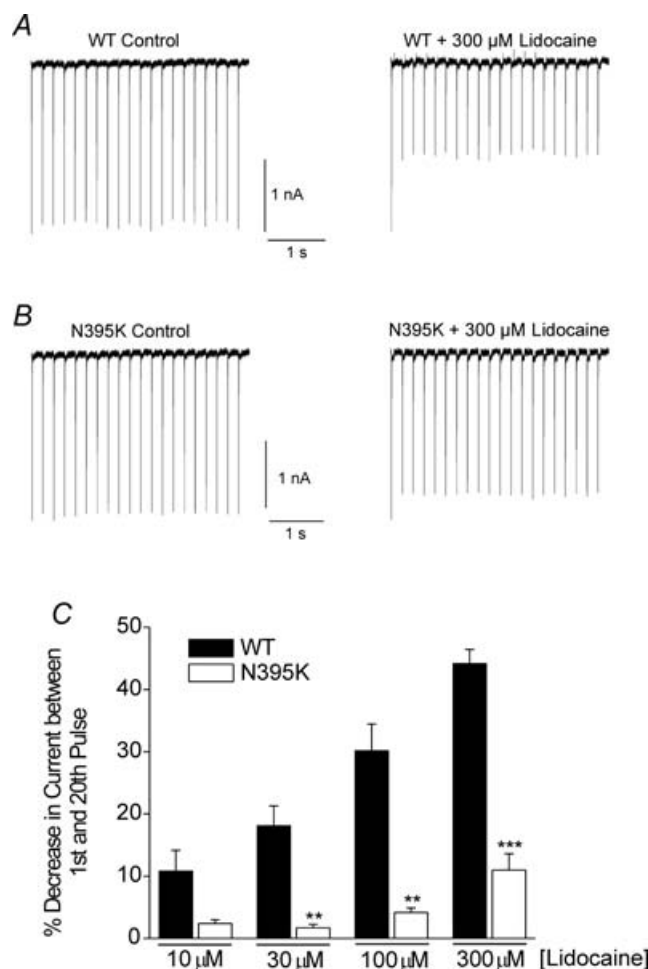


Figure 6. Use-dependent inhibition of WT and N395K current by lidocaine

A, example of peak WT currents during high frequency stimulation under control conditions (left) and in the presence of 300 μM lidocaine (right). **B**, example of peak N395K currents during high frequency stimulation under control conditions (left) and in the presence of 300 μM lidocaine (right). **C**, ratio of peak WT and N395K currents from the first pulse to the last pulse of the high frequency stimulation protocol in the presence of different concentrations of lidocaine. Data are presented as mean percentage decrease in current between the 1st and 20th pulse \pm s.e.m. (** $P < 0.01$, *** $P < 0.001$.)

Although the N395K mutation in Na_v1.7 showed resistance to lidocaine, it is possible that other hereditary erythromelalgia mutations outside of the local anaesthetic binding site might also alter lidocaine sensitivity. We therefore investigated the effects of lidocaine on Na_v1.7 containing another mutation (F216S) that has been identified in erythromelalgia patients (Drenth *et al.* 2005). A recent study shows that the F216S channel has a hyperpolarized voltage dependence of activation similar to the N395K mutation, but an enhanced steady-state slow inactivation (Choi *et al.* 2006). We examined the effects of 300 μ M and 1 mM lidocaine on inactivated F216S channels. These concentrations of lidocaine were chosen because both showed considerable inhibition of the WT channel in the inactivated (-50 mV pre-pulse) state. Figure 7A shows that the level of inhibition of inactivated F216S channels by 300 μ M ($38.4 \pm 2.1\%$, $n = 6$) and 1 mM ($58.2 \pm 2.5\%$; $n = 5$) were not significantly different from that of inactivated WT channels (300 μ M: $39.9 \pm 7.3\%$, $n = 11$; 1 mM: $55.9 \pm 4.9\%$, $n = 9$; Student's unpaired *t* test). However, inhibition of inactivated F216S channels by 300 μ M lidocaine and 1 mM lidocaine was significantly ($P < 0.001$) higher than inhibition of N395K channels by 300 μ M ($12.4 \pm 1.3\%$, $n = 6$) and 1 mM lidocaine ($26.2 \pm 4.2\%$, $n = 8$; Student's unpaired *t* test; Fig. 7A). We also investigated use-dependent inhibition of F216S currents by 300 μ M lidocaine by pulsing cells transfected with F216S to -10 mV at a frequency of 5 Hz in the presence of lidocaine. Figure 7B shows that F216S current amplitude decreased $42.7 \pm 2.5\%$ ($n = 6$) from the first pulse to the last pulse of the protocol in the presence of 300 μ M lidocaine and was not significantly different from the decrease seen with WT channels ($42.7 \pm 2.0\%$, $n = 11$; one-way ANOVA followed by a Tukey's comparison test). This decrease in F216S current amplitude was significantly ($P < 0.001$) higher than the decrease in N395K current amplitude ($11.0 \pm 2.6\%$, $n = 5$; one-way ANOVA followed by a Tukey's comparison test) induced by 300 μ M lidocaine (Fig. 7B). These data show that a hereditary erythromelalgia mutation outside of the Na_v1.7 local anaesthetic binding site does not affect the lidocaine sensitivity of Na_v1.7.

Discussion

In this study we showed that the N395K mutation in Na_v1.7 implicated in the painful inherited neuropathy hereditary erythromelalgia (Drenth *et al.* 2005) alters the voltage dependence of activation and steady-state slow inactivation as well as the kinetics of deactivation. A computer model of a sensory neuron expressing N395K channel properties displayed a decreased threshold for firing an action potential and a higher firing frequency in response to a range of current injections that had little effect on the WT sensory neuron model. Furthermore, the

N395 residue is homologous to residues found in the local anaesthetic binding site of other voltage-gated sodium channels, and we demonstrate that the N395K mutation attenuates the inhibitory effects of lidocaine on inactivated and resting Na_v1.7. This mutation also attenuates the use-dependent inhibition of lidocaine that was observed for wild-type Na_v1.7. Finally we demonstrate that a hereditary erythromelalgia mutation (F216S) outside of the Na_v1.7 local anaesthetic binding site that also alters voltage-dependent properties did not have effects on lidocaine inhibition.

The first goal of this study was to examine electrophysiological differences in Na_v1.7 caused by the N395K mutation. The hyperpolarizing shift in activation and slower onset of deactivation caused by N395K is similar to findings involving other hereditary erythromelalgia mutations (Cummins *et al.* 2004; Han *et al.* 2006; Harty *et al.* 2006). All of the other erythromelalgia mutations studied to date (F216S, S241T, I848T, L858H, L858F, F1449V and A863P) shift the voltage dependence of activation in the negative direction by 7–14 mV (Cummins *et al.* 2004; Dib-Hajj *et al.* 2005; Choi *et al.* 2006; Han *et al.* 2006; Harty *et al.* 2006; Lampert *et al.* 2006). All of the mutations, with the exception of F1449V, also

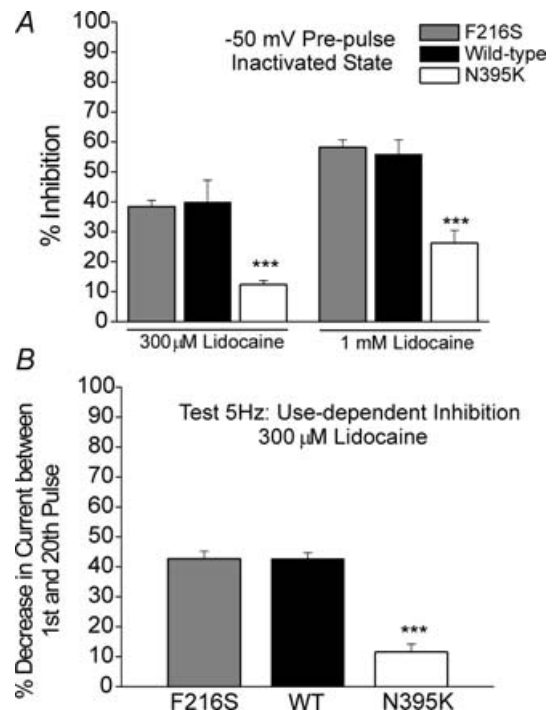


Figure 7. Inhibitory effects of lidocaine on the F216S channel compared to 1.7 WT and N395K

A, lidocaine (300 μ M and 1 mM) inhibition of inactivated F216S channels compared to inactivated WT channels and to inactivated N395K channels. B, ratio of peak F216S currents from the first pulse to the last pulse of the high frequency stimulation protocol in the presence of 300 μ M lidocaine compared to that of WT and N395K channels.

slow deactivation, but they differ in the manner in which they affect deactivation. The N395K mutation, like the F216S mutation, simply shifts the voltage dependence of the deactivation time constant curve in the negative direction in a manner that is consistent with the shift in activation. By contrast many of the other mutations, such as the L858H mutation, alter deactivation in a more pronounced voltage-dependent fashion (see Fig. 1D of Cummins *et al.* 2004). This suggests that the different erythromelalgia mutations alter Na_v1.7 gating in at least two distinct ways. The N395K mutation also caused impairment of steady-state slow inactivation which is seen with sodium channel mutations associated with disorders such as epilepsy and hyperkalaemic periodic paralysis, as well as hereditary erythromelalgia (Cummins & Sigworth, 1996; Bendahhou *et al.* 1999, 2002; Cummins *et al.* 2004; Rhodes *et al.* 2005). However, only the I848T and N395K erythromelalgia mutations impair slow inactivation. The F1449V mutation does not alter slow inactivation and the other mutations enhance slow inactivation. This differential effect on slow inactivation might indicate that slow inactivation may not be important for the pathophysiology of erythromelalgia.

Interestingly, a recent study (Fertleman *et al.* 2006) reported that three mutations linked to PEPD, a familial rectal pain syndrome, do not cause a hyperpolarizing shift in activation, but rather impair fast inactivation. It is intriguing that Na_v1.7 mutations predominantly associated with rectal pain may consistently impair fast inactivation while mutations predominantly associated with burning pain sensations in the hands and feet cause a hyperpolarizing shift in activation. It is not known if the PEPD mutations alter deactivation or slow inactivation of Na_v1.7. A total of eight different missense mutations were identified in families with PEPD but it is not known if all eight mutations alter predominantly fast inactivation or if any of the PEPD mutations increase excitability of sensory neurons.

To examine the relative impact of the changes in activation and slow inactivation associated with erythromelalgia mutations on neuronal excitability, we performed simulations using the NEURON computer program (Hines & Carnevale, 1997). Our simulations indicate that the shift in activation is sufficient to decrease the threshold for action potential generation and increase repetitive firing rates, changes that have been observed when recombinant F1449V, L858H, and A863P sodium channels were transfected into cultured DRG neurons (Dib-Hajj *et al.* 2005; Harty *et al.* 2006; Rush *et al.* 2006). The simulations also indicated that while changes in slow inactivation may not have major influences on neuronal excitability by themselves, they can significantly modulate the degree to which the shift in activation impacts excitability. These data suggest that mutations with impaired slow inactivation are more likely to be associated

with a severe clinical phenotype. The HH formulations used in the simulations presented here are not adequate to determine whether the differential effects of the mutations on deactivation kinetics can also modulate excitability and therefore we did not address this in the present study. Nonetheless, these results, based on observations of a hereditary erythromelalgia mutation, may provide insight into how electrophysiological changes in Na_v1.7 contribute to pain in humans. For example, our findings should help in determining whether changes in Na_v1.7 properties caused by modulation (e.g. phosphorylation) are likely to cause increased sensitization of nociceptive neurons and contribute to increased pain sensations.

The second goal of this study was to determine whether the N395K mutation changes the effects of lidocaine on Na_v1.7 current. The N395 residue is located in the S6 segment of domain I and lies within the local anaesthetic-binding site of Na_v1.7. One study has shown that lidocaine relieved pain in only 55% of erythromelalgia patients (Davis & Sandroni, 2005). This raises the possibility that specific mutations such as N395K in Na_v1.7 might render patients relatively unresponsive to lidocaine treatment. Therefore, our hypothesis was that mutation of this residue would reduce the inhibitory effects of lidocaine on channel current. Interestingly, we observed a two-phase inhibition of lidocaine on 1.7 WT-inactivated channels. The dose–response curve for this inhibition was best fitted by using a two-site binding model. One possibility for this phenomenon is that holding the cell at -50 mV for prolonged periods of time transitions a subset of channels into a high affinity binding state and a subset into a low affinity binding state. These two distinct states could involve closed-state and open-state inactivation which may have different affinities for lidocaine. A recent study in the giant squid axon showed that at -50 mV total inactivation is comprised of both closed-state and open-state inactivation (Armstrong, 2006). The possibility that the ratio of closed-state *versus* open-state inactivated channels during the prolonged -50 mV pre-pulse might explain the two-phase dose–inhibition curve for lidocaine on 1.7 WT-inactivated channels, while outside the scope of our current study, deserves further investigation. Nonetheless, our data clearly demonstrate an attenuation of lidocaine inhibition on inactivated N395K channels at -50 mV. This reduction of the lidocaine effect was seen at all concentrations tested including concentrations comparable to total lidocaine serum concentrations (~ 10 – 16 μ M) that have been shown to cause analgesia in neuropathic pain patients (Ferrante *et al.* 1996).

One explanation for the reduction of the lidocaine effect on the N395K channel is that the mutation impairs steady-state slow inactivation and thus there are fewer channels in the inactivated state. This could decrease the number of channels that preferentially bind lidocaine. Indeed, based on recordings from *Xenopus* oocytes,

Chevrier *et al.* (2004) proposed that lidocaine might alter slow inactivation of Na_v1.7 channels. However, F216S channels display enhanced steady-state inactivation at -50 mV (Choi *et al.* 2006) and in the present study, F216S channels did not show enhanced inhibition with lidocaine in the inactivated state compared to wild-type. Furthermore, WT channels pre-pulsed to -70 mV for 30 s and N395K channels pre-pulsed to -50 mV for 30 s both have approximately 21% of their channels slow inactivated (Fig. 1C), yet WT channels still displayed a higher inhibition of channel current by lidocaine with a -70 mV pre-pulse than N395K channels with a -50 mV pre-pulse (data not shown). This indicates that the N395K mutation in Na_v1.7 alters the direct interaction of lidocaine with the inactivated state of the channel, and suggests that changes in steady-state slow inactivation do not affect lidocaine inhibition of the channel. In addition, the inhibitory effect of lidocaine at high concentrations on the resting N395K channel was reduced compared to the resting WT channel. This further confirms that the N395K mutation affects the direct interaction of lidocaine with Na_v1.7 because the percentage of total channels in the resting state would be the same for N395K and WT using a -140 mV pre-pulse.

A recent study has reported that a loss of functional Na_v1.7 channels in humans due to homozygous nonsense mutations leads to a complete inability to sense pain (Cox *et al.* 2006). Surprisingly, individuals with this profound inability to sense pain were deemed to be healthy in virtually every other way. Although Na_v1.7 is believed to be present in both sensory and sympathetic ganglion neurons, none of the individuals studied by Cox *et al.* exhibited symptoms of autonomic nervous system dysfunction. As non-nociceptive sensory functions appeared normal in the individuals with the homozygous nonsense mutations that eliminated functional Na_v1.7 currents, the study by Cox *et al.* indicates that drugs that specifically target Na_v1.7 could have the potential to selectively ameliorate pain. It is important to note that the individuals studied by Cox *et al.* (2006) were all children between the ages of 6 and 14, so it is not yet clear if they have a complete inability to develop neuropathic pain. It has been reported that mice that selectively lack Na_v1.7 in their sensory neurons can develop neuropathic pain (Nassar *et al.* 2004) suggesting that Na_v1.7 may not be essential for neuropathic pain. However, mice that have a global deficit in Na_v1.7 die just after birth (Nassar *et al.* 2004), indicating that the role(s) of Na_v1.7 could be different between mice and humans. Although there is now clear evidence that at least two types of chronic painful neuropathies, hereditary erythromelalgia and PEPD, can be caused by mutations in SCN9A that alter the gating properties of Na_v1.7, it is not known if Na_v1.7 is important in other human chronic pain syndromes. Drugs that specifically block Na_v1.7 currents could help determine if Na_v1.7 channels play a major

role in common neuropathic pain syndromes such as diabetic neuropathy or pain associated with post-herpetic neuralgia.

Our results suggest that variability in the response of erythromelalgia patients to local anaesthetics that target sodium channels may be due, at least in part, to differing effects of the various hereditary erythromelalgia mutations in Na_v1.7 on lidocaine sensitivity. Our data predict that the pain symptoms in individuals with the N395K mutation are likely to be more intense and more resistant to lidocaine treatment than for individuals with the F216S mutation. Genotype–phenotype correlations are needed to help determine if this is indeed the case. Although none of the other hereditary erythromelalgia mutations identified thus far are located in the local anaesthetic-binding site, the possibility that one or more of these also alters lidocaine sensitivity merits examination in future experiments. Interestingly, all of the hereditary erythromelalgia mutations studied to date, including the N395K mutation studied here, induce a hyperpolarizing shift in the voltage dependence of activation of Na_v1.7 currents, suggesting that this alteration is crucial to the development of the pain associated with hereditary erythromelalgia. We speculate that other manipulations, such as phosphorylation, that also induce hyperpolarizing shifts in activation may also contribute to increased pain sensations. Thus our observations on the N395K mutation provide insight into the changes in Na_v1.7 channel activity that may contribute to abnormal pain sensations in erythromelalgia. Our results also suggest that research focusing on the function and pharmacology of the Na_v1.7 channel is crucial to the understanding of pain pathophysiology and the advancement of pain management therapies.

References

- Armstrong CM (2006). Na channel inactivation from open and closed states. *Proc Natl Acad Sci U S A* **103**, 17991–17996.
- Bendahhou S, Cummins TR, Kula RW, Fu YH & Ptacek LJ (2002). Impairment of slow inactivation as a common mechanism for periodic paralysis in DIIS4-S51. *Neurology* **58**, 1266–1272.
- Bendahhou S, Cummins TR, Tawil R, Waxman SG & Ptacek LJ (1999). Activation and inactivation of the voltage-gated sodium channel: role of segment S5 revealed by a novel hyperkalaemic periodic paralysis mutation. *J Neurosci* **19**, 4762–4771.
- Black JA, Dib-Hajj S, McNabola K, Jeste S, Rizzo MA, Kocsis JD & Waxman SG (1996). Spinal sensory neurons express multiple sodium channel alpha-subunit mRNAs. *Brain Res Mol Brain Res* **43**, 117–131.
- Chen Y, Yu FH, Surmeier DJ, Scheuer T & Catterall WA (2006). Neuromodulation of Na⁺ channel slow inactivation via cAMP-dependent protein kinase and protein kinase C. *Neuron* **49**, 409–420.

- Chevrier P, Vijayaragavan K & Chahine M (2004). Differential modulation of Nav1.7 and Nav1.8 peripheral nerve sodium channels by the local anesthetic lidocaine. *Br J Pharmacol* **142**, 576–584.
- Choi J, Dib-Hajj S & Waxman SG (2006). Inherited erythromelgia: Limb pain from an S4 charge-neutral Na channelopathy. *Neurology* **67**, 1–5.
- Cox JJ, Reimann F, Nicholas AK, Thornton G, Roberts E, Springell K, Karbani G, Jafri H, Mannan J, Raashid Y, Al-Gazali L, Hamamy H, Valente EM, Gorman S, Williams R, McHale DP, Wood JN, Gribble FM & Woods CG (2006). An SCN9A channelopathy causes congenital inability to experience pain. *Nature* **444**, 894–898.
- Cummins TR, Dib-Hajj SD, Black JA, Akopian AN, Wood JN & Waxman SG (1999). A novel persistent tetrodotoxin-resistant sodium current in SNS-null and wild-type small primary sensory neurons. *J Neurosci* **19**, RC43.
- Cummins TR, Dib-Hajj SD & Waxman SG (2004). Electrophysiological properties of mutant Nav1.7 sodium channels in a painful inherited neuropathy. *J Neurosci* **24**, 8232–8236.
- Cummins TR, Howe JR & Waxman SG (1998). Slow closed-state inactivation: a novel mechanism underlying ramp currents in cells expressing the hNE/PN1 sodium channel. *J Neurosci* **18**, 9607–9619.
- Cummins TR & Sigworth FJ (1996). Impaired slow inactivation in mutant sodium channels. *Biophys J* **71**, 227–236.
- Cummins TR & Waxman SG (1997). Downregulation of tetrodotoxin-resistant sodium currents and upregulation of a rapidly repriming tetrodotoxin-sensitive sodium current in small spinal sensory neurons after nerve injury. *J Neurosci* **17**, 3503–3514.
- Davis MD & Sandroni P (2005). Lidocaine patch for pain of erythromelgia: follow-up of 34 patients. *Arch Dermatol* **141**, 1320–1321.
- Dib-Hajj SD, Rush AM, Cummins TR, Hisama FM, Novella S, Tyrrell L, Marshall L & Waxman SG (2005). Gain-of-function mutation in Nav1.7 in familial erythromelgia induces bursting of sensory neurons. *Brain* **128**, 1847–1854.
- Djoughri L, Newton R, Levinson SR, Berry CM, Carruthers B & Lawson SN (2003). Sensory and electrophysiological properties of guinea-pig sensory neurones expressing Nav_v1.7 (PN1) Na⁺ channel α subunit protein. *J Physiol* **546**, 565–576.
- Drenth JP, te Morsche RH, Guillet G, Taieb A, Kirby RL & Jansen JB (2005). SCN9A mutations define primary hereditary erythromelgia as a neuropathic disorder of voltage gated sodium channels. *J Invest Dermatol* **124**, 1333–1338.
- Featherstone DE, Fujimoto E & Ruben PC (1998). A defect in skeletal muscle sodium channel deactivation exacerbates hyperexcitability in human paramyotonia congenita. *J Physiol* **506**, 627–638.
- Ferrante FM, Paggioli J, Cherukuri S & Arthur GR (1996). The analgesic response to intravenous lidocaine in the treatment of neuropathic pain. *Anesth Analg* **82**, 91–97.
- Fertleman CR, Baker MD, Parker KA, Moffatt S, Elmslie FV, Abrahamsen B, Ostman J, Klugbauer N, Wood JN, Gardiner RM & Rees M (2006). SCN9A mutations in paroxysmal extreme pain disorder: allelic variants underlie distinct channel defects and phenotypes. *Neuron* **52**, 767–774.
- Gold MS, Shuster MJ & Levine JD (1996). Characterization of six voltage-gated K⁺ currents in adult rat sensory neurons. *J Neurophysiol* **75**, 2629–2646.
- Han C, Rush AM, Dib-Hajj SD, Li S, Xu Z, Wang Y, Tyrrell L, Wang X, Yang Y & Waxman SG (2006). Sporadic onset of hereditary erythromelgia: a gain-of-function mutation in Nav_v1.7. *Ann Neurol* **59**, 553–558.
- Harty TP, Dib-Hajj SD, Tyrrell L, Blackman R, Hisama FM, Rose JB & Waxman SG (2006). Nav_v1.7 mutant A863P in erythromelgia: effects of altered activation and steady-state inactivation on excitability of nociceptive dorsal root ganglion neurons. *J Neurosci* **26**, 12566–12575.
- Hines ML & Carnevale NT (1997). The NEURON simulation environment. *Neural Comput* **9**, 1179–1209.
- Hodgkin AL & Huxley AF (1952). A quantitative description of membrane current and its application to conduction and excitation in nerve. *J Physiol* **117**, 500–544.
- Lampert A, Dib-Hajj SD, Tyrrell L & Waxman SG (2006). Size matters: Erythromelgia mutation S241T in Nav1.7 alters channel gating. *J Biol Chem* **281**, 36029–36035.
- Nassar MA, Stirling LC, Forlani G, Baker MD, Matthews EA, Dickenson AH & Wood JN (2004). Nociceptor-specific gene deletion reveals a major role for Nav 1.7 (PN1) in acute and inflammatory pain. *Proc Natl Acad Sci USA* **101**, 12706–12711.
- Nau C & Wang GK (2004). Interactions of local anesthetics with voltage-gated Na⁺ channels. *J Membr Biol* **201**, 1–8.
- Nau C, Wang SY, Strichartz GR & Wang GK (1999). Point mutations at N434 in D1-S6 of μ 1 Na⁺ channels modulate binding affinity and stereoselectivity of local anesthetic enantiomers. *Mol Pharmacol* **56**, 404–413.
- Rhodes TH, Vanoye CG, Ohmori I, Ogiwara I, Yamakawa K & George AL Jr (2005). Sodium channel dysfunction in intractable childhood epilepsy with generalized tonic-clonic seizures. *J Physiol* **569**, 433–445.
- Rush AM, Dib-Hajj SD, Liu S, Cummins TR, Black JA & Waxman SG (2006). A single sodium channel mutation produces hyper- or hypoexcitability in different types of neurons. *Proc Natl Acad Sci U S A* **103**, 8245–8250.
- Sangameswaran L, Fish LM, Koch BD, Rabert DK, Delgado SG, Ilnicka M, Jakeman LB, Novakovic S, Wong K, Sze P, Tzoumaka E, Stewart GR, Herman RC, Chan H, Eglén RM & Hunter JC (1997). A novel tetrodotoxin-sensitive, voltage-gated sodium channel expressed in rat and human dorsal root ganglia. *J Biol Chem* **272**, 14805–14809.
- Toledo-Aral JJ, Moss BL, He ZJ, Koszowski AG, Whisenand T, Levinson SR, Wolf JJ, Silos-Santiago I, Halebouga S & Mandel G (1997). Identification of PN1, a predominant voltage-dependent sodium channel expressed principally in peripheral neurons. *Proc Natl Acad Sci U S A* **94**, 1527–1532.
- van Genderen PJ, Michiels JJ & Drenth JP (1993). Hereditary erythromelgia and acquired erythromelgia. *Am J Med Genet* **45**, 530–532.
- Wang Y, Nicol GD, Clapp DW & Hingtgen CM (2005). Sensory neurons from Nf1 haploinsufficient mice exhibit increased excitability. *J Neurophysiol* **94**, 3670–3676.
- Wang GK, Russell C & Wang SY (2004). State-dependent block of voltage-gated Na⁺ channels by amitriptyline via the local anesthetic receptor and its implication for neuropathic pain. *Pain* **110**, 166–174.

Wang SY & Wang GK (1997). A mutation in segment I–S6 alters slow inactivation of sodium channels. *Biophys J* **72**, 1633–1640.

Yang Y, Wang Y, Li S, Xu Z, Li H, Ma L, Fan J, Bu D, Liu B, Fan Z, Wu G, Jin J, Ding B, Zhu X & Shen Y (2004). Mutations in *SCN9A*, encoding a sodium channel alpha subunit, in patients with primary hereditary erythromelalgia. *J Med Genet* **41**, 171–174.

Acknowledgements

This work was supported by National Institutes of Health Research Grant NS053422 (T.R.C.), the Paul and Carole Stark

Fellowship (P.L.S.), and the Medical Research Service and Rehabilitation Research Service, Department of Veterans Affairs, and by grants from the National Multiple Sclerosis Society and the Erythromelalgia Association (S.G.W.).

Supplemental material

Online supplemental material for this paper can be accessed at: <http://jp.physoc.org/cgi/content/full/jphysiol.2006.127027/DC1> and <http://www.blackwell-synergy.com/doi/suppl/10.1113/jphysiol.2006.127027>

A Nav1.7 channel mutation associated with hereditary erythromelalgia contributes to neuronal hyperexcitability and displays reduced lidocaine sensitivity

Patrick L. Sheets, James O. Jackson, II, Stephen G. Waxman, Sulayman D. Dib-Hajj and Theodore R. Cummins

J. Physiol. 2007;581;1019-1031; originally published online Apr 12, 2007;

DOI: 10.1113/jphysiol.2006.127027

This information is current as of June 16, 2008

Updated Information & Services	including high-resolution figures, can be found at: http://jp.physoc.org/cgi/content/full/581/3/1019
Supplementary Material	Supplementary material can be found at: http://jp.physoc.org/cgi/content/full/jphysiol.2006.127027/DC1
Subspecialty Collections	This article, along with others on similar topics, appears in the following collection(s): Neuroscience http://jp.physoc.org/cgi/collection/neuroscience
Permissions & Licensing	Information about reproducing this article in parts (figures, tables) or in its entirety can be found online at: http://jp.physoc.org/misc/Permissions.shtml
Reprints	Information about ordering reprints can be found online: http://jp.physoc.org/misc/reprints.shtml